Please cite the Published Version

Data Access Statement: The data that support the findings of this study are available from the corresponding author upon reasonable request.

Check for updates

Dipstick Sensor Based on Molecularly Imprinted Polymer-Coated Screen-Printed Electrodes for the Single-Shot Detection of Glucose in Urine Samples—From Fundamental Study toward Point-of-Care Application

Manlio Caldara,* Joseph W. Lowdon, Gil van Wissen, Alejandro Garcia-Miranda Ferrari, Robert D. Crapnell, Thomas J. Cleij, Hanne Diliën, Craig E. Banks, Kasper Eersels, and Bart van Grinsven

Glucose biosensors play an extremely important role in health care systems worldwide. Therefore, the field continues to attract significant attention leading to the development of innovative technologies. Due to their characteristics, Molecularly Imprinted Polymers (MIPs) represent a promising alternative to commercial enzymatic sensors. In this work, a low-cost, flexible MIP-based platform for glucose sensing by integrating MIP particles directly into screen-printed electrodes (SPEs) is realized. The sensor design allows the detection of glucose via two different transducer principles, the so-called "heat-transfer method" (HTM) and electrochemical impedance spectroscopy (EIS). The sensitivity and selectivity of the sensor are demonstrated by comparing the responses obtained toward three different saccharides. Furthermore, the application potential of the MIP-SPE sensor is demonstrated by analyzing the response in urine samples, showing a linear range of 14.38–330 μм with HTM and 1.37–330 μм with EIS. To bring the sensor closer to a real life application, a handheld dipstick sensor is developed, allowing the single-shot detection of glucose in urine using EIS. This study illustrates that the simplicity of the dipstick readout coupled with the straightforward manufacturing process opens up the possibility for mass production, making this platform a very attractive alternative to commercial glucose sensors.

M. Caldara, J. W. Lowdon, G. van Wissen, T. J. Cleij, H. Diliën, K. Eersels, B. van Grinsven
Sensor Engineering Department
Faculty of Science and Engineering
Maastricht University
Maastricht 6200 MD, the Netherlands
E-mail: m.caldara@maastrichtuniversity.nl
A. G.-M. Ferrari, R. D. Crapnell, C. E. Banks
John Dalton Building
Faculty of Science and Engineering
Manchester Metropolitan University
Chester Street, Manchester M1 5GD, UK

1. Introduction

Diabetes (or Diabetes mellitus) is considered a global burden both in terms of health-related and economic costs. According to the WHO, the number of people suffering from diabetes rose worryingly from 108 million in 1980 to 422 million in 2014, and in 2019, the disease was the direct cause of 1.5 million fatalities.[1] Inevitably, the cost for diabetic care multiplied, the American Diabetes Association (ADA) estimated a 26% increase in the total cost of diagnosed diabetes from $245 billion in 2012 to $327 billion in 2017 the United States only.[2] Diabetes is an incurable chronic disease that occurs when the pancreas does not produce enough insulin or when the body is not able to properly utilize the produced insulin.[3] The insulin-deficiency causes elevated levels of glucose in blood (also called hyperglycemia) as well as in other body fluids.[4–6] Therefore, the easiest and fastest way for the diagnosis and monitoring of diabetes are accomplished via the use of sensors able to quantify the glucose levels in physiological fluids. Unsurprisingly, the first glucose biosensor was developed by Leland Clark over 60 years ago in order to tackle the disease by allowing its early diagnosis. As diabetes still represents a condition that can lead to serious long-term health problems, the development of novel glucose biosensors continues to be one of the top priorities globally.[7,8] Generally, the recognition elements utilized in most commercial glucose sensors are represented by enzymes such as glucose oxidase (GOx) or glucose-1-dehydrogenase (GDH).[8,9] Despite the fact that these enzymes have extensively proven their reliability for glucose sensing over the last decades, their main limitations reside in their relatively short long-term stability,[10,11] loss of activity at extreme pH,[12] or reactivity toward other sugars (especially for GDH-based sensors).[13] For this reason, non-enzymatic glucose sensor have gained increasing attention from the scientific community in recent years.[14,15] A promising category

**ADVANCED
SCIENCE NEWS**

www.advancedsciencenews.com

**ADVANCED
MATERIALS
INTERFACES**

www.advmatinterfaces.de

of non-enzymatic recognition elements that could overcome the above-mentioned issues are molecularly imprinted polymers (MIPs).[16,17] MIPs are artificially synthesized materials with tailor-made binding cavities complementary to the template molecule in shape, size, and chemical functionalities; as such they are able to specifically and selectively bind to the target.[18] Some of the key advantages of these polymers are their high stability to extreme conditions, extremely long shelf life, and low-cost preparation methods.[19–21] MIPs have been successfully integrated into several platforms with the aim to detect a wide variety of targets, ranging from small organic molecules[22,23] to proteins,[24,25] viruses,[26] and bacteria.[27,28] These features make MIPs ideal candidates as recognition elements in glucose biosensors and for the analysis in complex matrices, such as physiological fluids.[29] In order to develop a promising alternative to commercial sensors, the key features that a glucose biosensor needs to address are cost-effectiveness and possibility of mass production. In addition, these techniques should be minimally or non-invasive to create a commercial edge over the traditional glucose meters that require the collection of blood using a lancet device. In the past years, many MIP-based sensors have been developed for glucose detection,[30,31] with most of them being MIP films polymerized onto a substrate[30,32–34] or platforms based on MIP micro particles embedded onto an adhesive layer.[35,36] Even though such sensors showed promising results in terms of sensitivity and selectivity, the materials and procedures used to develop the platforms make the production process highly difficult to reproduce on a large scale and difficult to implement in a clinical setting.

This research therefore focuses on the facile and up scalable fabrication of a MIP-modified screen-printed electrode for glucose detection and its potential for monitoring the glucose concentration in physiological samples. To this extent, MIP particles were prepared using a bulk polymerization approach employing a procedure optimized in the previous work,[35] the obtained particles were then mixed with carbon-graphitic ink and the mixture was screen-printed on top of the working electrode. This simple and straightforward procedure allowed the preparation of MIP-modified SPEs (MIP-SPEs) (**Figure 1**a) in a cost-effective and reproducible manner.

Moreover, the design of the fabricated platform made it possible to use the sensor with two different transducer technologies (Figure 1b,c), the heat-transfer method (HTM) and electrochemical impedance spectroscopy (EIS). The MIP-SPE platform was characterized with Scanning Electron Microscopy (SEM) and Cyclic Voltammetry (CV) to assess morphological characteristic and electrochemical behavior of the developed sensing platform. Then, HTM and EIS rebinding analysis in buffer solutions proved the specificity of the platform when compared to the reference control. The selectivity of the developed platform was proven by comparing the thermal response of the platform to different structural analogues of the target. Finally, the response of the MIP-SPE platform to untreated urine samples, spiked with glucose, was assessed via HTM and EIS analysis. To bring the technology closer to a market-ready application, the EIS sensor was transformed into a dipstick technology for the single-shot detection of glucose in urine samples (Figure 1c). The
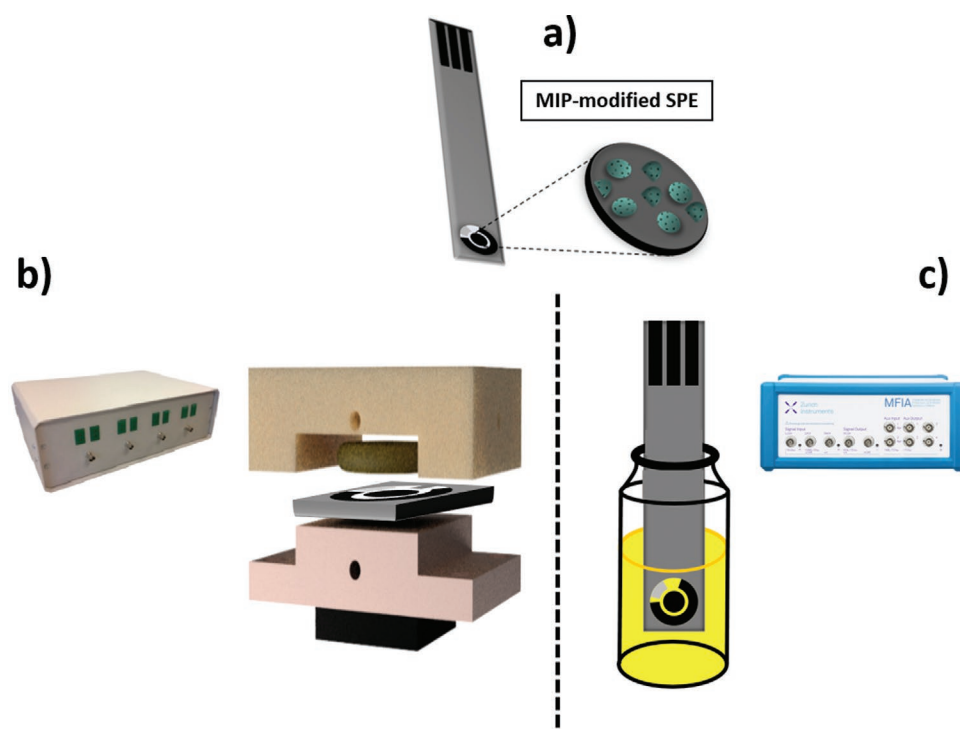

Figure 1. a) Design of the fabricated molecularly imprinted polymer-screen-printed electrode (MIP-SPE). b) Heat-transfer method (HTM) setup and c) Electrochemical impedance spectroscopy (EIS) setup adopted for rebinding analysis using MIP-SPE as dipstick technology.

ADVANCED
SCIENCE NEWS
www.advancedsciencenews.com

ADVANCED
MATERIALS
INTERFACES
Open Access
www.advmatinterfaces.de

results obtained in this paper illustrate that it is possible to accurately measure the glucose concentration in urine in a fast manner, further emphasizing its potential use in diabetes diagnosis and management.

2. Results and Discussion

2.1. SEM and CV Characterization of Functionalized MIP-SPE

The morphology of the functionalized part (working electrode) of the sensor was studied via Scanning Electron Microscopy (SEM) analysis (**Figure 2**). When analyzing the image obtained with the bare SPE, a flat and relatively smooth surface can be observed (Figure 2a). A different pattern is evident in the SEM image of MIP-SPE (Figure 2b). In fact, the modification of the electrode with graphitic ink and MIP micro particles can be clearly seen as the surface appears more rough and uneven when in presence of the polymer particles.

The electrochemical behavior of the functionalized SPEs was analyzed by CV voltammetry using a $[Fe(CN)_6]^{3-/4-}$ redox probe in KCl. In Figure 2c, cyclic voltammograms of MIP-SPE and NIP-SPE (red and blue lines) show increased oxidation and reduction peaks compared with those obtained for bare SPE (black line); the difference is attributed to the fabrication process of the modified SPEs, in which MIP-modified graphitic ink is screen-printed onto the working electrode. This results in an increased conductivity of the substrate due to the higher concentration of graphite in the WE. Another indication of the increased surface area in the modified electrodes is provided by the analysis of the oxidation peaks of the different

SPEs;[37] in fact, a shift from +0.4 to +0.37 V is observed when comparing the bare SPE with the MIP- and NIP-modified SPEs.

2.2. Heat-Transfer Rebinding Analysis in PBS

To scrutinize the rebinding efficiency of the MIP-modified SPEs thoroughly using the Heat-Transfer Method, the functionalized substrates were placed inside a flow cell at a stringently controlled temperature of 37.00 °C and upon injection of increasing concentrations of glucose in buffer solutions (PBS), the thermal variations at the solid–liquid interface were recorded and analyzed (**Figure 3**a). In order to get a direct comparison with the NIP-functionalized SPE and bare SPE and therefore assess the specificity of the MIP-SPE over the two reference materials, the obtained temperature values were baselined and then transformed to effect size (%) values using an equation reported in previous works (Figure 3b).[35] The data show a clear distinction in the temperature profiles of MIP-SPE (black lines), NIP-SPE (red lines), and Bare SPE (green lines) from the first analyte injection. This difference is seen to increase with higher concentrations of glucose, proving the specificity of the MIP-sensor in the entire analyzed range. The results are in line with results obtained in other studies and can be explained by the fact that when the target binds to the polymeric interface, the thermodynamic properties of the interfacial layer change. In this case, binding of glucose to the MIP layer, increases the thermal resistance of the interface, leading to a drop in temperature in the liquid flow cell above the MIP-functionalized sensor chip.[21,35,36]
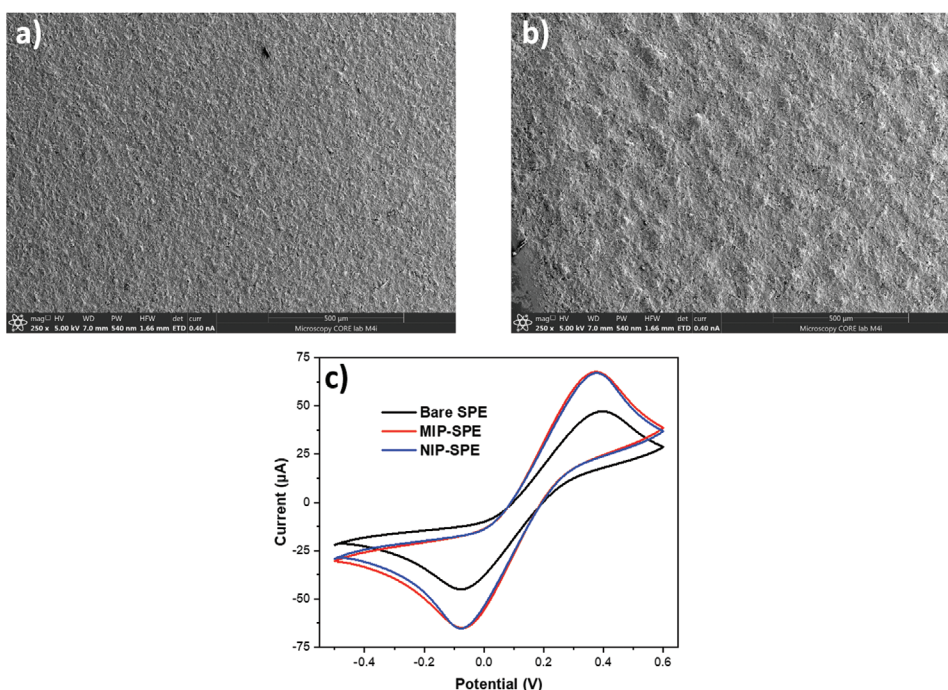

Figure 2. Characterization of the MIP-modified screen-printed electrodes. Scanning electron microscopy (SEM) images of working electrode of a) bare screen-printed electrode and b) screen-printed electrode modified with MIP particles (MIP-SPE). c) CV voltammograms of bare SPE, MIP-SPE, and NIP-SPE.
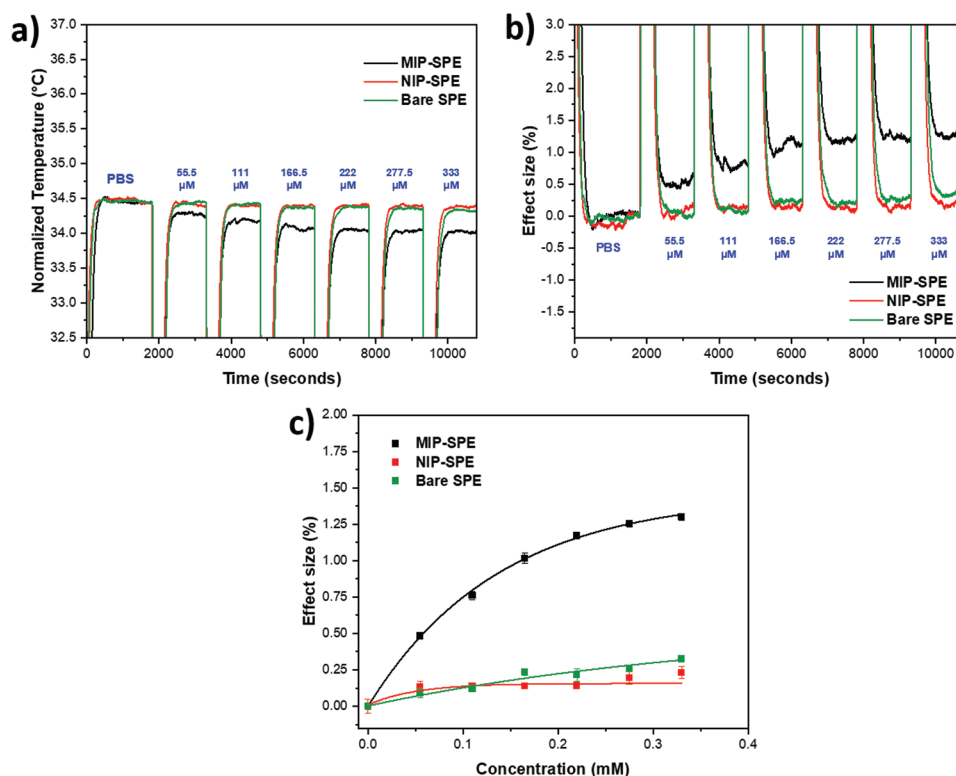
**ADVANCED
SCIENCE NEWS**
www.advancedsciencenews.com

**ADVANCED
MATERIALS
INTERFACES**
Open Access
www.advmatinterfaces.de

Figure 3. HTM rebinding analysis of MIP/NIP/Bare SPE after injection of glucose (55.5–333 µM). Analysis on time of a) Temperature and b) effect size changes upon injection of the analyte. c) Dose-response curves of MIP-SPE, NIP-SPE, and bare SPE.

Dose-response curves were constructed by plotting the effect size (%) values against the glucose concentration introduced inside the flow cell (Figure 3c). The dose-response curve obtained for the MIP-electrode shows a saturation trend commonly observed for imprinted polymers coupled with HTM as readout technology. In fact, the measurement shows a clear response after the first injections, which then starts to plateau due to the saturation of the binding sites available for the binding. For this reason, the data was fit asymptotically with Origin, version 2021b (OriginLabs Corporation, Northampton, MA, USA) for MIP-SPE ($R^2 = 0.9992$), NIP-SPE ($R^2 = 0.6297$), and Bare SPE ($R^2 = 0.9632$).

2.3. Electrochemical Impedance Spectroscopy (EIS) Rebinding Analysis in PBS

To further prove the specificity of the MIP-SPE substrate and demonstrate its versatility in detecting glucose with different readout technologies, an EIS rebinding analysis in phosphate-buffered solution (used to mimic physiological samples) was carried out (**Figure 4**). The analysis was carried out by connecting the functionalized SPEs to an impedance analyzer with a commercially available SPE connector, demonstrating then the potential of the modified electrode as sensing element in handheld electrochemical devices. The measurement was recorded after simply inserting the sensing part of the functionalized electrode into a vial containing increasing concentration of target (55.5–333 µM). The obtained data show that MIP-SPE

retains a high specificity when compared with NIP-SPE with a commercial electrochemical readout. A clear decrease in the absolute value of the impedance can be observed for the MIP-SPE after submerging it in the lowest concentration of glucose (Figure 4a,c); in contrast, it can be seen that the NIP-SPE shows a negligible change in the impedance value upon exposure to glucose solutions. Dose-response curves were constructed after baselining the absolute impedance values for MIP- and NIP-SPE, and then plotting the changes (delta Abs Z) against the glucose concentrations used for the analysis (Figure 4d). The MIP-modified electrode shows a linear behavior (black line, $R^2 = 0.9882$) with no evidence of saturation effects, suggesting that the sensor might be effective also at higher glucose concentrations when analyzed in PBS samples; NIP-SPE (red line, $R^2 = 0.9114$) instead shows a diminished response that seems to plateau with higher glucose levels.

2.4. Selectivity Studies of MIP-SPE

A key feature that needs to be evaluated for molecularly imprinted polymers and for biosensors in general is the selectivity of the sensor platform to a determined target over other competitors. To accurately assess the selectivity of the MIP-SPE substrate, the HTM response to three different saccharides was recorded and analyzed (**Figure 5**). One of the tested molecules is fructose, a simple sugar with the same molecular formula as glucose ($C_6H_{12}O_6$) and, as such, the two molecules are classified as functional isomers. However, when analyzing the structures
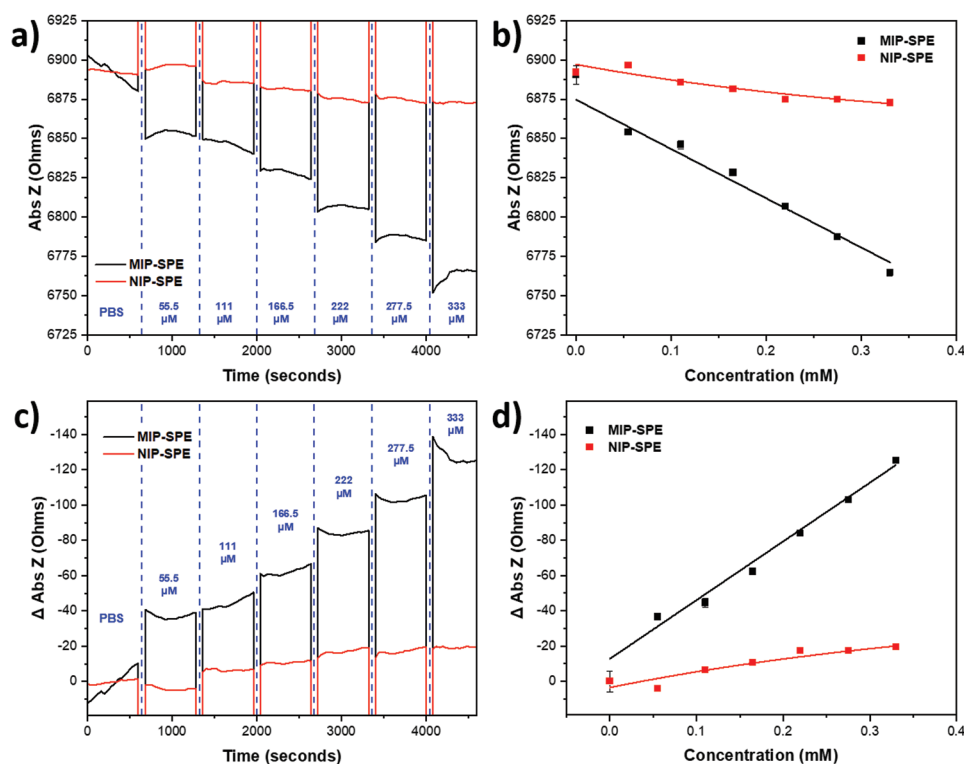
Figure 4. EIS rebinding analysis after injection of glucose (55.5–333 μm). Analysis on time of a) Absolute *Z* values and b) Delta absolute *Z* at different concentrations of glucose. Dose-response curves for MIP-SPE and NIP-SPE of c) Absolute *Z* and d) Delta absolute Z.

of these two molecules, glucose is a six-membered ring, while fructose is a five-membered ring. Thus, it can be deducted that this structural difference is responsible for the clearly higher response of the sensor to glucose in comparison to fructose (Figure 5c). The other molecules tested (sucrose and lactose) instead are made up of two monosaccharides, and therefore are classified as disaccharides. It is important to highlight that both the molecules contain one glucose unit in their structure and as such are good indicator of the MIP selectivity. Despite this structural similarity, the developed MIP-SPE sensor exhibits high specificity (Figure 5a,b) and selectivity (Figure 5c) toward glucose over these molecules, thus suggesting that size and shape of the analyzed disaccharides obstruct the potential interactions with the MIP-modified electrode.

2.5. Rebinding Analysis in Urine Samples via HTM and EIS Analysis

The potential applicability of the developed sensor for glucose detection in physiological samples was proven via HTM and EIS analysis of untreated urine samples spiked with the target. From the raw data measurements obtained with the two different readout technologies it can be clearly observed a distinctive change for the MIP-SPE substrate, whereas NIP-SPE shows little to no response with both HTM and EIS (**Figure 6**a,c). Specifically, in the HTM analysis of the MIP-SPE, a decrease in temperature is observed after each injection of the glucose solutions due to the obstruction of the heat flow at the solid–liquid

interface as a result of the interaction between the target and the cavities present in the polymer. The NIP-SPE signal, on the other hand, shows very little change after injections, thereby proving the specificity of the MIP sensor. To better highlight and compare the thermal response of MIP- and NIP-modified SPE, dose-response curves were constructed as indicated above (Figure 6b), and the data were fitted asymptotically for both MIP-SPE (black line, $R^2 = 0.9905$) and NIP-SPE (red line, $R^2 = 0.9356$).

Although HTM is commercially interesting due to its low-cost and user-friendly operating mechanism, its application in handheld single-shot analysis of urine samples, similar to a blood glucose meter, is cumbersome with the current equipment. Therefore, an EIS-based sensor was developed using a handheld commercial SPE connector and a commercial impedance analyzer. This device can be used as a dipstick for non-invasive single-shot glucose detection in urine. The sensor was "dipped" in urine samples, spiked with the same concentrations analyzed by the HTM method, therefore allowing a direct comparison between the two different data sets. The results show a clear decrease in the absolute value of the impedance upon exposure of the MIP-functionalized SPE to the lowest concentration of glucose, whereas the reference NIP-SPE shows a much smaller decrease. Furthermore, the change in impedance increases linearly when the MIP sensor is placed in contact with higher concentrations of glucose, thus demonstrating the reliability of the designed SPE for the quantitative analysis of glucose in complex matrices such as urine. To make interpretation of the impedance changes of MIP- and NIP-modified SPE
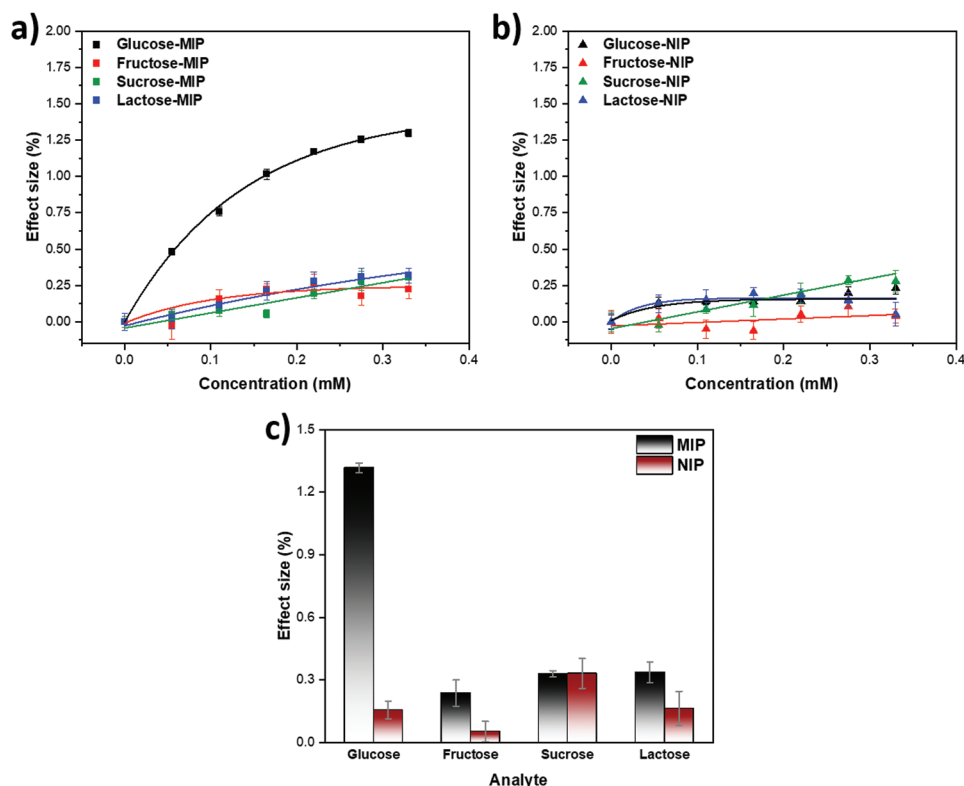
ADVANCED
SCIENCE NEWS
www.advancedsciencenews.com

ADVANCED
MATERIALS
INTERFACES
Open Access
www.advmatinterfaces.de

Figure 5. Selectivity studies via HTM analysis. Dose-response curves obtained after exposing a) MIP-SPE and b) NIP-SPE to increasing concentrations of three different saccharides. c) Analysis of the MIP-SPE/NIP-SPE response (%) after exposure to 0.33 mM of glucose, fructose, sucrose, and lactose.

during the rebinding experiments easier, dose-response curves for MIP-SPE (black line, $R^2 = 0.9861$) and NIP-SPE (red line, $R^2 = 0.8017$) were constructed in Figure 6d. When analyzing the constructed curves with both the transducers (Figure 6), it is clear that the MIP-sensor can be successfully employed for both HTM and EIS analysis in a complex physiological matrix, such as urine. The sensitivity of the developed sensor in urine samples was assessed by calculating the limit of detection (LoD) from the dose-response curves of MIP-SPE (Figure 6b,d, black lines). The LoD was calculated using the three-sigma rule, (blue dashed line) corresponding to the maximum noise value of the signal throughout the measurement multiplied by three. The obtained y-values were then plotted (blue lines) and their intercept with the MIP-fits allowed the calculation of the two LoDs. The calculated LoDs were found to be 14.38 μM for the HTM and 1.37 μM for the EIS urinalysis. These results demonstrate the potential of MIP-SPE as low-cost, diagnostic device for the non-invasive diagnosis of diabetes in urine samples as the sensor proves its efficiency in the physiologically relevant regime. Moreover, when comparing Figures 3 and 4 with Figure 6, it can be seen that the sensor's performance is not highly affected from complex matrices and therefore might be further developed for glucose detection in different body fluids.

3. Conclusion

In this work, we have successfully prepared an imprinted polymer for glucose detection using a free radical bulk

polymerization approach. The prepared MIP particles were then employed as recognition element to fabricate a MIP-functionalized screen-printed electrode (MIP-SPE) sensor. The MIP-SPE sensor was fabricated by simple screen-printing a mixture of graphitic ink and MIP particles onto the working electrode of a standard carbon SPE. The sensor has demonstrated to be incredibly selective and is sensitive enough to allow both thermal and electrochemical quantification in urine samples in physiologically relevant concentrations. In terms of commercial application, the impedimetric sensor mainly stands out by the possibility of using it in combination with a handheld SPE connector and a commercial impedance analyzer in a dipstick configuration. This would allow for the single-shot, non-invasive analysis of the glucose concentration in urine samples. The low-cost, disposable nature of the chips makes this possible, while the impedimetric sensor enables end-users to quickly get a result that can be easily quantified. In the current setup we used a benchtop impedance analyzer but this can easily be replaced by a handheld model once implementation is complete. The combination with the easily scalable production process of the SPEs further emphasizes the commercial potential of the platform. Batch-to-batch variability resulting from the heterogeneity of the produced MIPs, has mainly shown to influence the baseline but not the relative response of the normalized MIP-NIP signal. For this specific application, in this concentration range, a simple baseline calibration correction would suffice to get rid of this batch-to-batch variability. However, a fully automated process that would allow for the mass production of large batches of homogenous, high-affinity MIPs
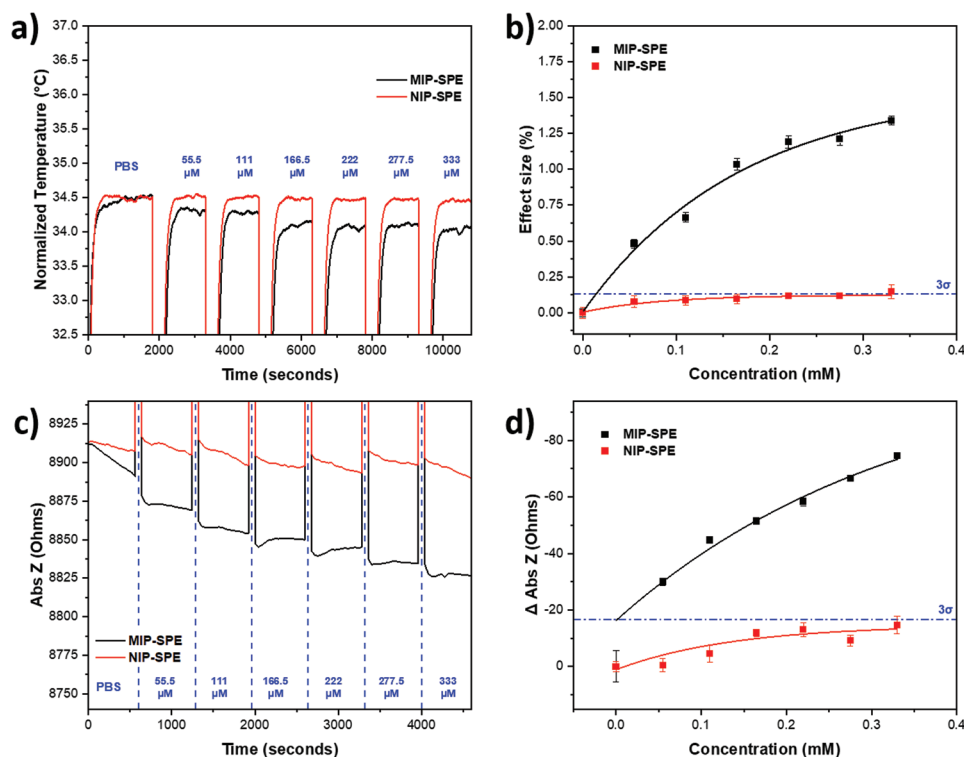
ADVANCED
SCIENCE NEWS
www.advancedsciencenews.com

ADVANCED
MATERIALS
INTERFACES
www.advmatinterfaces.de

Figure 6. HTM and EIS rebinding analysis in human urine samples. Raw data obtained via a) HTM and c) EIS analysis after exposing the MIP-/NIP-modified SPE sensor to increasing concentration of glucose. Dose-response curves constructed from b) HTM and d) EIS measurements, the blue dashed lines indicate the calculated LoDs (3σ method).

remains a topic that needs to be researched in order to further improve the applicability of the sensing platform.

4. Experimental Section

Materials: Stabilizers were removed from the monomer and cross-linker through filtration on aluminum oxide. Aluminum oxide (≥99.7%), acrylamide (≥99.9%), D-glucuronic acid (≥98%), D-glucose (≥99%), methanol (HPLC grade), acetic acid (≥99.8%), dimethyl sulfoxide (≥99.7%), potassium chloride (99%), potassium ferricyanide (≥99%), potassium ferrocyanide trihydrate (≥99%) were purchased from Fisher Scientific (Landsmeer, the Netherlands). Ethylene glycol dimethactrylate (≥98%) and azobisisobutyronitrile (≥98%) were purchased from Sigma Aldrich (Zwijndrecht, the Netherlands). Test strips for glucose analysis (Medi-Test) and Phosphate buffered saline (PBS) tablets 1X were obtained from VWR International BV (Amsterdam, the Netherlands). Milli-Q water (18.2 MΩ cm^{-1}) or phosphate-buffer saline (PBS) were used to prepare solutions for rebinding studies.

Preparation of Molecularly Imprinted Polymers: Bulk molecularly imprinted polymers (MIPs) for the detection of glucose were synthesized through free radical polymerization, following a procedure reported in the previous work with slight modifications.[35] A dummy imprinting approach was employed using glucuronic acid as template to enhance the interaction with the functional monomer (acrylamide) during the imprinting process. Briefly, D-glucuronic acid (97 mg), acrylamide (282 mg), ethylene glycol dimethacrylate (EGDMA, 1.13 mL), and azobisisobutyronitrile (AIBN, 50 mg) were dissolved in dimethyl sulfoxide (DMSO, 6 mL). The pre-polymerization solution was degassed with N$_2$ for 15 min, and then the polymerization was performed at 65 °C for 18 h. The bulk MIP was then ground and the obtained micro particles were dried at 65 °C overnight. The removal of the template was achieved employing a previously described procedure.[35] A reference control

(NIP) was prepared in parallel following the same procedure as per the MIP.

Fabrication of the Screen-Printed Macroelectrodes (SPEs) and Glucose-MIPs Bulk Modified Screen-Printed Macroelectrodes (MIP-SPEs): Stencil designs with a microDEK 1760RS screen-printing machine (DEK, Weymouth, UK) were used for the production of the SPEs. For each of the screen-printed electrodes, a carbon–graphite ink formulation was first screen-printed onto a polyester flexible film (Autostat, 250 μm thickness). After that, the layer was cured at 60 °C for 30 min in a box fan oven with extraction. Next, a silver/silver chloride (60:40) reference electrode was applied by screen-printing Ag/AgCl paste (Product Code: C2040308P3; Gwent Electronic Materials Ltd, UK) onto the plastic substrate. Then, this layer was cured at 60 °C for 30 min in an oven. Finally, an insulating dielectric paste ink (Product Code: D2070423D5; Gwent Electronic Materials Ltd, UK) was printed to cover the connections and define the 3.1 mm diameter graphite working electrode. One more time, this layer was cured in the same conditions as the previous layers. After these steps, the SPE are ready to use and these platforms have been well characterized in previous works.[38–41]

The glucose-MIPs modified screen-printed macroelectrodes (MIP-SPEs) were made by modifying the carbon–graphitic ink via modification with glucose-MIPs. This was carried out using a weight percentage of M$_P$ to M$_I$, where M$_P$ is the mass of particulate (the mass of glucose-MIPs) and M$_I$ is the total mass of the ink including the base graphitic ink and the mass of the particulate.[42–45] This was thoroughly mixed into the ink and screen-printed on top of the carbon–graphite working electrode.

The equation (M$_P$/M$_I$) × 100 was used to formulate the 5 wt% MIP-SPEs. A 5 wt% of glucose-MIPs was used to ensure consistent printing of the analyte in the fabrication process and to test viability of the proposed system. The screen-printed electrodes used throughout this work had a connection length of 32 mm and average resistance of 2.16 ± 0.06 kΩ.[46]

Scanning Electron Microscope (SEM) and Cyclic Voltammetry (CV) Characterization of Modified SPEs: In order to characterize the surface

**ADVANCED
SCIENCE NEWS**

www.advancedsciencenews.com

**ADVANCED
MATERIALS
INTERFACES**

www.advmatinterfaces.de

morphology of the modified screen-printed electrode, a bare SPE and a MIP-modified SPE were placed into 12 mm disks and after gold coating, the samples were imaged using a Scios Dualbeam scanning electron microscope (SEM). Cyclic voltammetry studies of bare SPE, NIP-SPE, and MIP-SPE were performed using a PalmSens4 potentiostat (PalmSens BV, Utrecht, the Netherlands). CV scans were recorded at a potential range of −0.5 to 0.6 V in 0.01 м $[Fe(CN)_6]^{3-/4-}$ (1:1) and 0.1 м KCl as electrolyte solution at a scan rate of 0.05 V s^{-1}.

Heat-Transfer Method (HTM) Setup: The sensing platform used for the HTM rebinding studies has been described in previous works.[47,48] Briefly, MIP-modified screen-printed electrodes were placed on a copper heat sink. The temperature of the sink, T_1, was strictly controlled using a K-type thermocouple (TC Direct, Nederweert, the Netherlands), a power resistor (Farnell, Utrecht, the Netherlands) and a software-based PID controller ($P = 10$, $I = 8$, $D = 0$) in Labview (National Instruments, Austin, TX, USA). The electrode was exposed to the different analytes using an injection-molded polycarbonate (PC) flow cell ($A = 28$ mm^2, $V = 110$ μL). A syringe pump was used to inject the studied samples at a rate of 0.250 mL min^{-1} for 5 min. To measure thermal changes at the solid–liquid interface, a second thermocouple monitored the temperature inside the flow cell, T_2, at a constant inlet temperature of 37 °C. To stabilize the signal, phosphate-buffered saline (PBS) or human urine solution was used. Increasing concentrations (55.5–333 μм) of glucose solutions (or competitor) were gradually injected into the system. To stabilize the signal, a waiting time of 20 min was observed between each addition. Mean values and error bars presented in all the HTM analysis are obtained from the average of three measurements.

Electrochemical Impedance Spectroscopy (EIS) Analysis: A MFIA impedance analyzer (Zurich Instruments, Zurich, Switzerland) was used to measure the impedance changes. The impedance analyzer was connected to the functionalized SPEs using a portable PalmSens SPE connector (PalmSens BV, Utrecht, the Netherlands). The sensing part of the modified screen-printed electrode was then inserted into vials containing 10 mL glucose solutions in PBS or untreated urine samples, ranging from 55.5 to 333 μм. Continuous frequency sweeps were taken at a low-frequency range from 10 Hz to 1 kHz at a test signal of 300 mV. Dose-response curves were obtained from the absolute impedance values at a single frequency at which the corresponding phase angle is 45°. Mean values and error bars presented in all the EIS studies are obtained from the average of three measurements.

HTM and EIS Analysis in Urine Samples: Human urine samples were collected from a healthy volunteer. The absence of glucose in the samples was confirmed using commercially available Medi-Test Glucose test strips. Increasing concentrations of glucose (55.5–333 μм) in urine samples were then prepared and employed for the HTM and EIS rebinding analysis with no need of additional pre-treatment of the physiological sample.

Conflict of Interest

The authors declare no conflict of interest.

Data Availability Statement

The data that support the findings of this study are available from the corresponding author upon reasonable request.

Keywords

dipstick sensors, molecularly imprinted polymers, non-enzymatic glucose sensors, non-invasive glucose monitoring, screen-printed electrodes

[1] World Health Organization, Diabetes, https://www.who.int/news-room/fact-sheets/detail/diabetes, **2022**.

[2] W. Yang, T. M. Dall, K. Beronjia, J. Lin, A. P. Semilla, R. Chakrabarti, P. F. Hogan, M. P. Petersen, *Diabetes Care* **2018**, *41*, 917.

[3] M. Karamanou, A. Protogerou, G. Tsoucalas, G. Androutsos, E. Poulakou-Rebelakou, *World J. Diabetes* **2016**, *7*, 1.

[4] Ö. Kap, V. Kılıç, J. G. Hardy, N. Horzum, *Analyst* **2021**, *146*, 2784.

[5] A. R. Naik, Y. Zhou, A. A. Dey, D. L. G. Arellano, U. Okoroanyanwu, E. B. Secor, M. C. Hersam, J. Morse, J. P. Rothstein, K. R. Carter, J. J. Watkins, *Lab Chip* **2022**, *22*, 156.

[6] K. L. Wolkowicz, E. M. Aiello, E. Vargas, H. Teymourian, F. Tehrani, J. Wang, J. E. Pinsker, F. J. Doyle, M. E. Patti, L. M. Laffel, E. Dassau, *Bioeng. Transl. Med.* **2021**, *6*, e10201.

[7] J. D. Newman, A. P. F. Turner, *Biosens. Bioelectron.* **2005**, *20*, 2435.

[8] Y. Zhang, J. Sun, L. Liu, H. Qiao, *J. Diabetes Its Complications* **2021**, *35*, 107929.

[9] M. H. Hassan, C. Vyas, B. Grieve, P. Bartolo, *Sensors* **2021**, *21*, 4672.

[10] H.-H. Fan, W.-L. Weng, C.-Y. Lee, C.-N. Liao, *ACS Omega* **2019**, *4*, 12222.

[11] M. Petruleviciene, J. Juodkazyte, I. Savickaja, R. Karpicz, I. Morkvenaite-Vilkonciene, A. Ramanavicius, *J. Electroanal. Chem.* **2022**, *918*, 116446.

[12] D.-W. Hwang, S. Lee, M. Seo, T. D. Chung, *Anal. Chim. Acta* **2018**, *1033*, 1.

[13] J. P. Frias, C. G. Lim, J. M. Ellison, C. M. Montandon, *Diabetes Care* **2010**, *33*, 728.

[14] D. B. Gorle, S. Ponnada, M. S. Kiai, K. K. Nair, A. Nowduri, H. C. Swart, E. H. Ang, K. K. Nanda, *J. Mater. Chem. B* **2021**, *9*, 7927.

[15] M. Wei, Y. Qiao, H. Zhao, J. Liang, T. Li, Y. Luo, S. Lu, X. Shi, W. Lu, X. Sun, *Chem. Commun.* **2020**, *56*, 14553.

[16] J. Wackerlig, P. A. Lieberzeit, *Sens. Actuators, B* **2015**, *207*, 144.

[17] O. S. Ahmad, T. S. Bedwell, C. Esen, A. Garcia-Cruz, S. A. Piletsky, *Trends Biotechnol.* **2019**, *37*, 294.

[18] F. Pessagno, M. Blair, M. J. Muldoon, P. Manesiotis, *ACS Appl. Polym. Mater.* **2022**, *4*, 7770.

[19] H. Chen, F. Wu, Y. Xu, Y. Liu, L. Song, X. Chen, Q. He, W. Liu, Q. Han, Z. Zhang, Y. Zhou, W. Liu, *RSC Adv.* **2021**, *11*, 29752.

[20] M. Kimani, E. Kislenko, K. Gawlitza, K. Rurack, *Sci. Rep.* **2022**, *12*, 14151.

[21] F. A. Tabar, J. W. Lowdon, M. Caldara, T. J. Cleij, P. Wagner, H. Diliën, K. Eersels, B. van Grinsven, *Environ. Technol. Innov.* **2023**, *29*, 103021.

[22] J. W. Lowdon, K. Eersels, R. Arreguin-Campos, M. Caldara, B. Heidt, R. Rogosic, K. L. Jimenez-Monroy, T. J. Cleij, H. Diliën, B. van Grinsven, *Molecules* **2020**, *25*, 5222.

[23] V. Ratautaite, E. Brazys, A. Ramanaviciene, A. Ramanavicius, *J. Electroanal. Chem.* **2022**, *917*, 116389.

[24] N. Bereli, M. Andaç, G. Baydemir, R. Say, I. Y. Galaev, A. Denizli, *J. Chromatogr. A* **2008**, *1190*, 18.

[25] D. Çimen, N. Bereli, S. Günaydın, A. Denizli, *Talanta* **2022**, *246*, 123484.

[26] G. M. Birnbaumer, P. A. Lieberzeit, L. Richter, R. Schirhagl, M. Milnera, F. L. Dickert, A. Bailey, P. Ertl, *Lab Chip* **2009**, *9*, 3549.

**ADVANCED
SCIENCE NEWS**

www.advancedsciencenews.com

**ADVANCED
MATERIALS
INTERFACES**

www.advmatinterfaces.de

[27] R. Arreguin-Campos, K. Eersels, J. W. Lowdon, R. Rogosic, B. Heidt, M. Caldara, K. L. Jiménez-Monroy, H. Diliën, T. J. Cleij, B. van Grinsven, *Microchem. J.* **2021**, *169*, 106554.

[28] B. Bräuer, M. Werner, D. Baurecht, P. A. Lieberzeit, *J. Mater. Chem. B* **2022**, *10*, 6758.

[29] M. Pirzada, E. Sehit, Z. Altintas, *Biosens. Bioelectron.* **2020**, *166*, 112464.

[30] E. Sehit, J. Drzazgowska, D. Buchenau, C. Yesildag, M. Lensen, Z. Altintas, *Biosens. Bioelectron.* **2020**, *165*, 112432.

[31] M. Caldara, J. Kulpa, J. W. Lowdon, T. J. Cleij, H. Diliën, K. Eersels, B. van Grinsven, *Chemosensors* **2023**, *11*, 32.

[32] S. J. Cho, H.-B. Noh, M.-S. Won, C.-H. Cho, K. B. Kim, Y.-B. Shim, *Biosens. Bioelectron.* **2018**, *99*, 471.

[33] C. Karaman, O. Karaman, N. Atar, M. L. Yola, *Microchim. Acta* **2022**, *189*, 24.

[34] A. Diouf, B. Bouchikhi, N. el Bari, *Mater. Sci. Eng., C* **2019**, *98*, 1196.

[35] M. Caldara, J. W. Lowdon, R. Rogosic, R. Arreguin-Campos, K. L. Jimenez-Monroy, B. Heidt, K. Tschulik, T. J. Cleij, H. Diliën, K. Eersels, B. van Grinsven, *ACS Sens.* **2021**, *6*, 4515.

[36] M. Frigoli, J. W. Lowdon, M. Caldara, R. Arreguin-Campos, J. Sewall, T. J. Cleij, H. Diliën, K. Eersels, B. van Grinsven, *ACS Sens.* **2023**, *8*, 353.

[37] M. Peeters, B. van Grinsven, C. Foster, T. Cleij, C. Banks, *Molecules* **2016**, *21*, 552.

[38] F. E. Galdino, C. W. Foster, J. A. Bonacin, C. E. Banks, *Anal. Methods* **2015**, *7*, 1208.

[39] J. P. Metters, R. O. Kadara, C. E. Banks, *Analyst* **2011**, *136*, 1067.

[40] A. A. Khorshed, M. Khairy, C. E. Banks, *Talanta* **2019**, *198*, 447.

[41] A. A. Khorshed, M. Khairy, C. E. Banks, *J. Electroanal. Chem.* **2018**, *824*, 39.

[42] J. P. Hughes, F. D. Blanco, C. E. Banks, S. J. Rowley-Neale, *RSC Adv.* **2019**, *9*, 25003.

[43] P. S. Adarakatti, M. Mahanthappa, J. P. Hughes, S. J. Rowley-Neale, G. C. Smith, S. Ashoka, C. E. Banks, *Int. J. Hydrogen Energy* **2019**, *44*, 16069.

[44] S. J. Rowley-Neale, C. W. Foster, G. C. Smith, D. A. C. Brownson, C. E. Banks, *Sustainable Energy Fuels* **2017**, *1*, 74.

[45] N. Srinivasa, L. Shreenivasa, P. S. Adarakatti, J. P. Hughes, S. J. Rowley-Neale, C. E. Banks, S. Ashoka, *RSC Adv.* **2019**, *9*, 24995.

[46] M. J. Whittingham, N. J. Hurst, R. D. Crapnell, A. Garcia-Miranda Ferrari, E. Blanco, T. J. Davies, C. E. Banks, *Anal. Chem.* **2021**, *93*, 16481.

[47] M. Caldara, J. W. Lowdon, J. Royakkers, M. Peeters, T. J. Cleij, H. Diliën, K. Eersels, B. van Grinsven, *Foods* **2022**, *11*, 2906.

[48] R. Arreguin-Campos, M. Frigoli, M. Caldara, R. D. Crapnell, A. G.-M. Ferrari, C. E. Banks, T. J. Cleij, H. Diliën, K. Eersels, B. van Grinsven, *Food Chem.* **2023**, *404*, 134653.